湖南大学学报（自然科学版）
Journal of Hunan University (Natural Sciences)

第 51 卷 第 6 期
2024 年 6 月

Available online at http://jonuns.com/index.php/journal/index

Vol. 51 No. 6
June 2024

Open Access Article

https://doi.org/10.55463/issn.1674-2974.51.6.32

Optimization of Graphene-Enhanced Geopolymer Cement for Oil Well Applications

Mohd Firdaus Habarudin[1,2,*], Nasir Shafiq[1], Afif Izwan Abd Hamid[1], Nurul Nazmin Zulkarnain[2], Ahmad Amirhilmi A Razak[2], and Siti Humairah A Rahman[2]

[1]Civil Engineering Department, Universiti Teknologi PETRONAS, Bandar Seri Iskandar, 32610 Perak, Malaysia.

[2]PETRONAS Research Sdn. Bhd., Kajang, 43000 Selangor, Malaysia

* Corresponding author: mfirdaus.habarudin@petronas.com

Received: May 12, 2024 / Revised: June 10, 2024 / Accepted: June 15, 2024 / Published: June 30, 2024

Abstract: Geopolymer cement is a viable and sustainable replacement for conventional Portland cement, drawing attention for its enhanced durability and reduced shrinkage compared to API Class G cement, along with its potential to reduce CO_2 emissions. This research aims to develop a fly-ash-based geopolymer cement incorporating graphene oxide (GO) under high-pressure, high-temperature (HPHT) conditions for oil-well cementing applications. The investigation proceeds in three distinct phases to meet its objectives. Initially, Phase 1 identified the optimal GO concentration as a strengthening additive in the geopolymer mixture. GO addition within certain concentrations, markedly improves compressive strength. Phase 2 focused on applying the optimal formulation (Formulation OP 1) in functional tests for oil well cementing, while Phase 3 assessed the effects of temperature and pressure on the compressive strength of Formulation OP 1 to simulate real-world downhole conditions. Higher temperatures increased compressive strength, likely due to accelerated geopolymerization and improved pore structure. Validation experiments confirmed the accuracy of the predictive models and demonstrated the robustness of Formulation OP 1 under varying conditions. This study highlights geopolymer cement's capability as a sustainable, high-performance option for challenging oil well settings, presenting a significant advancement over traditional oil well cement solutions.

Keywords: fly ash, alkaline activator ratio, carbon capture, utilization and storage (CCUS), compressive strength, central composite design.

石墨烯增强土聚物水泥在油井应用中的优化

摘要：地聚物水泥是传统波特兰水泥的可行且可持续的替代品，与 API G 级水泥相比，地聚物水泥具有更高的耐久性和更低的收缩性，并且具有减少二氧化碳排放的潜力，因此备受关注。本研究旨在开发一种在高压高温 (HPHT) 条件下加入氧化石墨烯 (GO) 的粉煤灰基地聚物水泥，用于油井固井应用。研究分为三个不同的阶段进行，以实现其目标。最初，第 1 阶段确定了地聚物混合物中作为强化添加剂的最佳 GO 浓度。在一定浓度内添加 GO 可显著提高抗压强度。第 2 阶段专注于将最佳配方（配方 OP 1）应用于油井固井功能测试，而第 3 阶段评估了温度和压力对配方 OP 1 抗压强度的影响，以模拟真实的井下条件。更高的温度会增加抗压强度，这可能是由于加速了地聚物反应并改善了孔隙结构。验证实验证实了预测模型的准确性，并证明了配方 OP 1 在不同条件下的稳健性。这项研究强调了土聚物水泥作为一种可持续、高性能选择的能力，适用于具有挑战性的油井环境，与传统油井水泥解决方案相比具有显著的进步。

关键词：粉煤灰，碱性活化剂比，碳捕获、利用和储存（CCUS），抗压强度，中心复合设计。

1. Introduction

Malaysia has traditionally relied on its oil and gas sector as a cornerstone of its energy industry since oil was discovered in Miri, Sarawak, in 1910. This discovery has attracted significant investment from major oil companies in both the upstream and downstream sectors, catalyzing economic transformation through job creation, skill development, and infrastructural advancement. However, concerns remain regarding the long-term safety and sustainability of existing and newly drilled wells. Ordinary Portland cement (OPC) API Class G has been traditionally used in oil and gas well applications because of its versatility [1]. This cement type's properties can be tailored with additives to suit various well conditions, including depth and temperature. However, its vulnerability to degradation, especially in the presence of sour gas, raises concerns about its long-term integrity in oil production environments. This has necessitated the exploration of more resilient materials. The reaction between API Class G cement and sour gas leads to disruption of the intergranular structure of the cement [2].

Geopolymer cement derived from industrial by-products like fly ash has emerged as a promising alternative. It boasts superior mechanical properties, enhanced durability, carbon dioxide (CO_2) and sulfate resistance, and low environmental impact [2]-[7]. The geopolymerization process creates a robust amorphous structure, which provides a solid foundation for oil-well cementing applications. Geopolymer cement is a type of inorganic adhesive that can be formed by combining minerals that contain high amounts of silica and alumina and then undergoing a polymerization process [8]. The primary alkaline chemicals commonly used to produce geopolymer cement include calcium hydroxide ($Ca(OH)_2$), sodium hydroxide (NaOH), sodium silicate (Na_2SiO_3), the combination of NaOH and Na_2SiO_3, the combination of potassium hydroxide (KOH) and NaOH, potassium silicate (K_2SiO_3) and its combination, and sodium carbonate ($NaCO_3$) [7], [9]-[10]. Sulfate activators such as sodium sulfate can also be used as alkaline activators. As found in [11], the use of such activators can increase ettringite formation, leading to a denser fly ash surface. Different combinations of alkaline solutions yield different strengths and features of geopolymer cements. Despite its potential, the current use of fly ash remains low, highlighting an opportunity for increased adoption in cement formulations. According to [12], the compressive strength of fly ash samples over an extended period shows minimal variance when cured in seawater compared to plain water. Therefore, the application of fly ash-based geopolymer cement in oil wells is deemed viable.

Prior studies have indicated that the potency of fly-ash-derived geopolymer cement can be enhanced by the addition of graphene [13]-[17]. The inclusion of these components in geopolymer cement serves to augment its strength, durability, and flexibility, enhance its resistance to aging, and improve the microstructure and stability of cement-based systems. Additionally, it helps to decrease the porosity of cement [13]-[16]. Graphene is a two-dimensional form of carbon consisting of a single layer of atoms bonded together through overlapping sp^2 hybrid bonds. These atoms are arranged in a hexagonal pattern resembling a honeycomb, with a thickness of just one atom. Andre Geim and Konstantin Novoselov discovered the quantum mechanics in 2004, which led them to receive the 2010 Nobel Prize in Physics [18]. Subsequently, scientists have extensively examined the features of graphene and its potential applications in batteries, transistors, computer chips, energy generation, supercapacitor, and the building industry. A chemical vapor deposition (CVD)-based process was employed to generate high-quality single-layer graphene flakes at reduced cost [18]. Graphene oxide (GO) is the preferred choice for most well-cementing formulations due to the presence of epoxy, hydroxyl (–OH), and –COOH groups in GO. The epoxy and hydroxyl groups were chemically bonded to the basal planes, whereas the carbonyl and carboxyl groups [were located at the margins [19]-[20]. These groups increase the distance between the layers, resulting in layers that are more water-attracting (hydrophilic) and therefore easily disperse in water [19]-[20].

Recent studies suggest that even minimal concentrations can significantly increase both the bending and compressive strength by 20% and 40%, respectively [21]. Further investigations by Udeze et al. [13] found that incorporating GO into the geopolymer mixture at levels between 0.013% and 0.053% reduced the compressive strength. This reduction was attributed to difficulties in achieving an even distribution and preventing clumping of the nanomaterial at high concentrations. As reported in [14], the optimal compressive strength was achieved at a GO concentration of 0.05%, whereas a GO concentration of 0.1% resulted in the weakest performance. This finding aligns with [15], which identified the most effective GO concentration for cement formulation to be 0.5% after seven days of curing and 0.1% after twenty-eight days. The effects of adding GO at concentrations of 0.01% to 0.10% to geopolymer cement were explored in [16], noting a significant improvement in the tensile strength. Similarly, experiments were conducted in [17] by incorporating 1%-4% GO into a geopolymer cement and observed that curing at room temperature for up to 60 days led to increased strength in both the initial and later stages. However, increasing the GO content from 3% to 4% diminished the compressive strength at all tested ages.

However, most of the studies, including those mentioned above, did not investigate the effects of those materials on geopolymer cements at low and high curing temperatures and under pressurized conditions to simulate well conditions. The extensive research on and

successful application of GO in the concrete industry highlight its potential as a beneficial additive. Given the similarities between concrete and well-cement in terms of their chemical and structural properties, the use of graphene oxide in well-cement is a promising approach for exploring and offering significant improvements in the performance of well-cement.

Due to the limited literature on the effect of GO in geopolymer well cement, the use of fly-ash-based geopolymer cement with GO as an oil-well cement is worth further investigation. By leveraging the existing body of research and proven effectiveness in the concrete industry, the incorporation of GO into well cement can lead to improvements such as improved rheological properties, reduced fluid loss, and optimum thickening times. The study contributes to understanding the behavior of this cement formulation, especially at high-pressure high-temperature (HPHT) conditions. The author hypothesizes that the incorporation of GO into the geopolymer cement mixture can enhance its compressive strength. Nevertheless, an optimal concentration of GO can be introduced before the strength begins to decline.

Hence, to find the GO optimum concentration, this study uses Response Surface Methodology (RSM) and Central Composite Design (CCD) to maximize the compressive strength of the cement. Analysis of variance was employed to evaluate the significance of the interaction factors and the experiment's validity. Response surface graphs were created for all investigated characteristics, and the substantial interaction effects for all identified features were assessed. The obtained optimal formulation was then subjected to oilwell cement testing, including rheology, fluid loss, and thickening time tests, according to American Petroleum Institute RP 10B-2 [22].

2. Materials and Methods

2.1. Materials

In this study, Class F pozzolanic fly ash from coal combustion was used. Fly ash was obtained from a licensed Tenaga Nasional Berhad Janamanjung power station located in Manjung, Perak, Malaysia. The chemical composition of the fly ash is detailed in Table 1.

Table 1 Oxide composition of Tanjung Bin fly ash (developed by the authors)

Element	SiO_2	Al_2O_3	Fe_2O	CaO	MgO	K_2O	SO_3	Na_2O	Others	Moisture	LOI
Weight (%)	39.1	18.4	9.44	13.4	7.56	1.48	1.97	8.2	<0.1	0.05	0.3

The geopolymerization process for the fly ash-based geopolymer uses an alkaline activator composed of sodium hydroxide (NaOH) and sodium silicate (Na_2SiO_3). A 50 wt.% (12.5 M) concentration of NaOH and liquid Na_2SiO_3 (containing 34.5-36.5% SiO_2 and 16.5-17.5% Na_2O) were acquired from Sigma-Aldrich. The sodium silicate solution was diluted to 50 wt.% using distilled water. Graphene oxide (GO), which was incorporated into the geopolymer cement formulation, was also procured from Sigma-Aldrich with a specification of 4 milligrams per milliliter (mg/ml) dispersed in water and a density of 0.981 g/mL. The graphene oxide was used as received without further purification. The elemental analysis of GO is provided in Table 2.

Table 2 Elemental analysis of GO (developed by the authors)

Element	Carbon	Hydrogen	Nitrogen	Sulfur	Oxygen
%	48-54	0-1	0-1	0-2	42-51

2.2. Methods

2.2.1. Test Matrices Design

The study was conducted in three distinct (3) phases; (1) identifying the optimal graphene oxide (GO) concentration, (2) evaluating the performance of the optimal formulation in oil-well cement functional tests, and (3) analyzing the impact of varying temperatures and pressures on the geopolymer cement's compressive strength using the optimal formulation. A statistical design of experiment (DOE), Response Surface Methodology (RSM) of Central Composite Design (CCD) by Design Expert software version 13 was employed to design the test matrices for Phases 1 and 3. The CCD approach was used to generate mathematical models from the experimental data prior to establishing the optimal geopolymer formulation. The $NaOH/Na_2SiO_3$ ratio was kept constant at 1:1 throughout the study. In order to assess the reliability and precision of the established model, analysis of variance (ANOVA) was performed. The R-squared (R^2) value was calculated to confirm the reliability of the generated models. Using Fisher's *F*-test, the statistical significance of the produced model was determined, and the *p*-value (probability of error) was used to assess the model coefficients. Tables 3 and 4 present the test matrices for Phases 1 and 3, respectively. For Phase 2, the geopolymer cement with the optimal GO concentration underwent oil-well cement functional tests, including rheology, fluid loss, and thickening time tests.

For Phase 1, the factors were NaOH molarity and GO concentration. The NaOH molarity was set within a range of 3-5 M to ensure that the geopolymer slurry remained workable, while the GO concentration varied from 0 to 0.2% by weight of fly ash (bwof). In the third phase, the experimental factors were the pressure and temperature, with the pressure and temperature settings ranging from 1,000 to 3,000 psi and 60 to 120°C.

Table 3 Test matrices for Phase 1 (developed by the authors)

Formulation	NaOH Molarity (M)	GO Concentration (%bwof)	Compressive Strength (psi)
1	3	2	2957
2	4	1.1	2664
3	4	1.1	2739
4	2.6	1.1	1507
5	4	2.4	2281
6	4	1.1	2813
7	3	0.2	1988
8	5	2	1828
9	4	0	1395
10	4	1.1	2391
11	4	1.1	2635
12	5.4	1.1	1144
13	5	0.2	2713

Table 4 Test matrices for Phase 3 (developed by the authors)

Formulation	Pressure (psi)	Temperature (°C)	Compressive Strength (psi)
1	2000	132	3204
2	1000	60	1047
3	3000	60	1051
4	586	90	2264
5	2000	90	2394
6	3414	90	2336
7	1000	120	3171
8	3000	120	3795
9	2000	90	2426
10	2000	90	2253
11	2000	90	2358
12	2000	48	1038
13	2000	90	2307

2.2.2. Geopolymer Cement Mixing Process

The preparation of the geopolymer cement with the GO admixture was performed according to the procedures outlined in API RP 10B-2 [23]. The chemical components were precisely measured using a scale to ensure accuracy. The GO solution was subjected to sonication for 1 hour before mixing to enhance its dispersion. An Ametek Chandler Constant Speed Mixer was used for the blending process, beginning with the addition of seawater to the mixer cup. After adding seawater, the mixer was activated at a speed of 4,000 RPM to achieve a consistent mixing rate. This was followed by gradual addition of 50 wt.% NaOH solution and stirring for 60 seconds to promote the initial dissolution and interaction among the components. Next, 50 wt.% Na_2SiO_3 solution was introduced and mixed for an additional 60 seconds, facilitating the chemical processes required for geopolymerization. After ensuring that the liquid ingredients were well mixed, fly ash was added to the mixture, followed by stirring for another 60 seconds to evenly distribute the solid particles. The predetermined amount of GO was then incorporated into the mixture. To complete the mixing operation and ensure a uniform mixture of all components, the mixing speed was increased to 12,000-RPM for 35 seconds. This final step of intense mixing is crucial for eliminating agglomerates and obtaining a smooth, consistent slurry that is ready for subsequent testing procedures.

2.2.3. Geopolymer Cement Curing Process

Before the mixing process, 2" x 2" x 2" cubic mold was greased and prepared. Once the mixing process has been completed, the geopolymer slurry is immediately poured into the mold. The curing process occurred in a pressure-temperature chamber, adhering to the guidelines outlined in API RP 10B-2, as illustrated in Fig. 1. The curing conditions were a pressure of 3000 psi and a temperature of 90°C, maintained for 24 hours. The pressure condition is following the Petronas Technical Guideline (PTG) for cementing Clause 9.4.3.2, while the temperature condition was simulating 85% of the bottom-hole static temperature (BHST) of the well [24]. Prior to 24 h of curing, the samples were remolded and immersed in a water-cooling bath at room temperature for 45 min. To evaluate the compressive strength, a dedicated API Compressive Strength Tester (Fig. 2) was employed to conduct the test on the cement cube. The loading rate was set to 4,000 psi/min per API RP 10B-2 guidelines.

Fig. 1 Pressurized HPHT curing chamber (provided by the authors)

Fig. 2 API Compressive strength tester (provided by the authors)

2.2.4. Rheology of the Geopolymer Slurry

This evaluation focused on the rheological attributes of the geopolymer cement mixed with GO, employing a viscometer to determine shear stress versus shear strain, apparent viscosity, plastic viscosity, and yield point. The rheological tests were executed both at ambient and 90°C using a Fann VG Viscometer Model 35A (FANN® Instrument Company, as shown in Fig. 3a. The geopolymer slurry was subjected to shearing by two components: an external rotating sleeve (the rotor) and an internal fixed cylinder (the bob), as depicted in Fig. 3b. The rotor was set to operate at various fixed speeds, while the bob, which was attached to the torsion spring, deflected in reaction to the torque generated by the slurry's viscosity. Throughout the test, for each slurry composition, six dynamic viscosity readings were systematically obtained at rotational speeds of 300, 200, 100, 6, and 3 rpm.

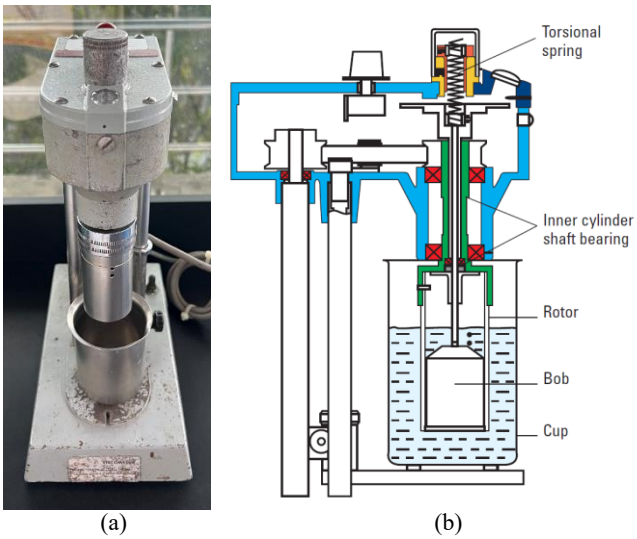

(a) (b)

Fig. 3 (a) Viscometer (Model 35A, FANN®) and (b) Schematic drawing of a co-axial cylinder viscometer [22].

The stress curves were fitted by the Herschel-Bulkley (H-B) model as shown in Eq. (1) below:

$$\tau = \tau_y + K\gamma^n \quad (1)$$

which use three rheological parameters: the Herschel-Bulkley yield stress (τ), the flow consistency index (K), and the flow behavior index (n), which indicates whether the fluid exhibits shear thinning or shear thickening behavior [25]-[27]. The H-B model, also known as the yield power law model, is a methodology for delineating the characteristics of certain viscous fluids. This model is particularly suited to fluids exhibiting yield stress, where the shear stress is adhered to a power law model under increased shear rates [27].

2.2.5. Fluid Loss of Geopolymer Slurry

Fluid loss tests were performed to evaluate the filtration of cement at 90°C under differential pressure conditions using a CTE HPHT Filter Press, as shown in Fig. 4. After the mixing process, the geopolymer slurry was conditioned using an atmospheric consistometer for 30 minutes. Concurrently, a fluid loss cell was prepared by fitting it with the required accessories. After slurry conditioning, the slurry was immediately poured into the fluid loss cell. To ensure that the top stem valve was sealed, the cell was then positioned within the heating jacket. A nitrogen valve assembly was attached to the cell's top stem valve to supply pressure to the cell. The temperature inside the fluid loss cell was carefully monitored until it reached 90°C. A graduated cylinder was placed under the bottom stem valve to collect the filtrate when the desired temperature was reached. To mimic bottom-hole conditions, a differential pressure of 1,000 psi was applied. The procedure proceeded with partial opening of the bottom stem valve, starting with the timer immediately after the filtrate began to flow. The filtrate was collected over a period of 30 minutes.

Fig. 4 CTE HPHT filter press (provided by the authors)

Upon completion of the test, the volume of filtrate collected was doubled to calculate the API fluid loss in ml/30 minutes, adhering to standard reporting procedures. In instances where the experiment concludes prematurely, indicated by nitrogen expulsion (a hissing sound from the bottom stem valve), the test and timer are immediately halted. Both the filtrate volume and elapsed time were recorded. The API fluid loss in ml/30 min was then determined using Eq. (2):

$$API\ Fluid\ Loss = 2V_t\sqrt{\frac{30}{t}} \quad (2)$$

where V_t is the volume of filtrate collected at the time of blowout, and t is the blowout time in minutes.

2.2.6. Thickening Time of the Geopolymer Slurry

An API HPHT consistometer (Model 8340, Chandler Engineering) was used to assess the pumpability of the geopolymer slurry. The test is crucial for designing geopolymer formulations that remain pumpable under downhole conditions, thereby preventing premature hardening or curing. The thickening time is defined as the duration required for the geopolymer slurry to reach consistency within the range of 70-100 Bc. Immediately after mixing, the geopolymer slurry was transferred into an API slurry cup, which is a crucial step to maintain its initial fluidity and workability. Subsequently, the slurry was placed in the consistometer, where it was exposed to conditions of 3000 psi and 90°C to effectively simulate downhole environments.

3. Results and Discussion

3.1. Effect of GO Concentration on the Compressive Strength of Geopolymers

Phase 1 of the study investigated the optimal concentration of GO to be incorporated into the geopolymer cement to maximize its compressive strength. Based on the results presented in Table 3, a linear regression model was developed. The compressive strength experimental data for the NaOH molarity and GO concentration were fitted into the equation by analysis of variance (ANOVA). The ANOVA results for NaOH molarity and GO concentration are presented in Table 5. Eq. (3) expresses the empirical model of compressive strength (CS), which indicates the relationship between NaOH molarity and GO concentration in actual factors.

$$CS = 5851A + 1002B - 515AB - 675A^2 + 491B^2 - 9387 \quad (3)$$

where A represents the NaOH molarity and B represents the GO concentration.

Table 5 ANOVA results for the polynomial model in Eq. (3) (developed by the authors)

Response	Source	SS	DF	MS	*F*-value	*p*-value
Compressive Strength	Model	3.49×10^6	5	6.99×10^5	33.71	<0.0001
	Error	1.02×10^5	10	2.55×10^4		

*SS: Sum of squares; DF: Degree of freedom; MS: Mean square

ANOVA findings show that the obtained model gives very high R^2, adjusted R^2, and predicted R^2 values of 0.97, 0.94, and 0.94, respectively. Fig. 5 shows the predicted and actual compressive strength values. It can be seen that almost all points were distributed along a diagonal line, indicating that the predicted value conformed to the actual experimental values. Therefore, the obtained model provides a satisfactory estimation of the predicted values and can be used to predict compressive strength.

Fig. 6 presents contour and 3D response surface plots derived from the CCD analysis based on the effects of NaOH molarity and GO concentration on the compressive strength of fly ash-based geopolymer cement. The contour lines on the graph indicate regions of equal compressive strength, providing a visual representation of synergistic and antagonistic interactions between variables. The design points marked by red dots represent the central points of the experimental runs. The color gradient ranging from red to green indicates a transition from high compressive strength to low compressive strength. The plots show that an increase in NaOH molarity positively contributes to the compressive strength up to a certain level. However, beyond an optimum point, further increases in NaOH molarity may lead to a decrease in compressive strength, as indicated by the leveling off of the contour lines at higher molarities. An analysis of the contour lines revealed a peak compressive strength exceeding 3,000 psi within a middle-range NaOH molarity of approximately 4.5 M.

Similarly, the addition of GO at certain concentrations appeared to improve the compressive strength. This finding was in agreement to several other researchers [13]-[14], [17], [28]. It can be observed that

the inclusion of GO in as low as 0.2% bwof positively affected the compressive strength. The highest compressive strength, indicated by the deep red region, was observed at an intermediate NaOH molarity level and at high and low GO concentrations. Higher strengths were obtained due to the greater surface area and wrinkled morphology of the GO nanosheets. Due to this morphology, the interlocking mechanism within the geopolymer matrixes has been improved [14], [17], [29].

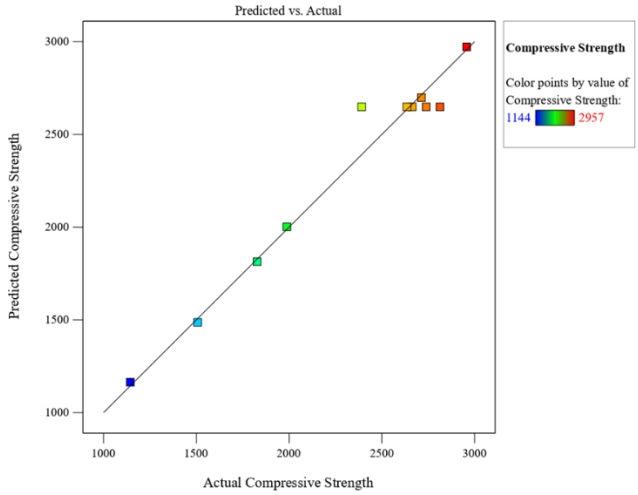

Fig. 5 Predicted versus actual values plotted by the Design Expert for the compressive strength of Phase 1 (developed by the authors)

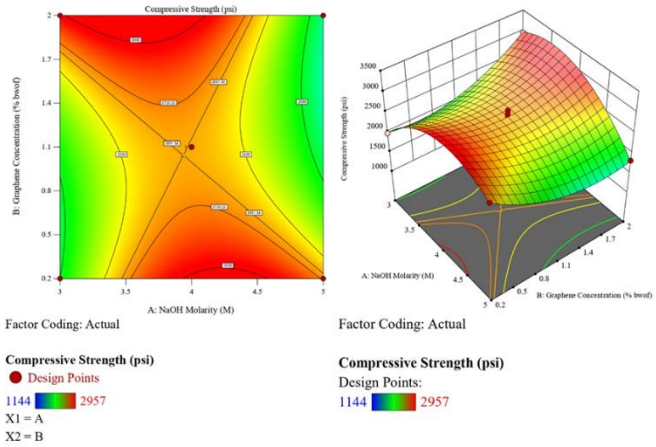

Fig. 6 Contour and 3D response surface plots from Design Expert for compressive strength versus NaOH molarity and GO concentration in Design Expert (developed by the authors)

The rounded edges of GO enhance its mechanical contact with the cementitious matrix. Chemical interactions between oxygen functional groups and hydration products are responsible for the formation of covalent bonds. As explained in [30] and [31], a chemical interaction takes place between the carboxylic acid of GO and the $Ca(OH)_2$ or C-S-H of the cementitious matrix. By directing the development spots and trends of the hydration products via the ‘‘template impact”, GO functions as a nucleating site for the hydration of cement [14]. Molecular mechanics simulations suggest that functional groups on the GO basal planes can substantially adhere to Ca^{2+} ions from the C-S-H [32]. Due to these factors, the bond between GO and the cement matrix was strengthened. This makes it easier for the stress to move from one place to another and increases the compressive strength of the geopolymer cement.

Yet, there is an optimal concentration range for GO, as excessive GO concentrations can negatively affect mechanical properties, as reflected in the lower compressive strength values in areas with higher GO concentrations. The lowest strength values, denoted by the outermost green region, correspond to the extreme ends of the design space, particularly at lower NaOH molarities (< 3.3 M) and low GO concentrations (< 1.6 %), where the strength decreases below 17.12 MPa (2,500 psi). In addition, the compressive strength value is also low when NaOH exceeds 4.5 M and the GO concentration exceeds 0.5% bwof. A decrease in the compressive strength at higher GO contents was observed due to the agglomeration of GO nanosheets in the geopolymer cement, which decreased the interfacial bond between the cement hydration [14], [17]. On the other hand, this reduction in compressive strength is associated with the adverse impact of higher dosages of GO that cause the dispersion of GO as a nanomaterial throughout the cement matrix, which is revealed to delay the appropriate action of GO in improving the strength of cement matrix [14]. Many studies have found that flocculated GO sheets are much less efficient than well-distributed GO sheets in improving the mechanical properties of cement matrix owing to the latter’s significant surface area consumption in boosting the hydration process via nuclei action [14], [17]. The optimal region indicates the best formulation for maximizing the compressive strength of the geopolymer cement under the studied conditions. The results of this analysis provide critical insights for the formulation of fly ash-based geopolymer cements, emphasizing the importance of the controlled addition of NaOH and GO to achieve a balance between workability and mechanical performance.

The optimization process was carried out after generating a well-fitted, accurate, and reliable compressive strength mathematical model. Table 6 summarizes the optimization data for Phase 1. Since the optimal formulation will be used for the next phase, which is oil-well functional testing, it is crucial to consider the workability and cost of the formulations. Thus, during the optimization process, both the NaOH molarity and the GO concentration were set in the range of 3–5 M and 0.2%–1.1% bwof, respectively. From the table, the established optimum NaOH molarity and GO concentration were 3.83 M NaOH and 0.2 % GO (Formulation OP 1). In this optimal formulation, the predicted compressive strength is 20.16 MPa (2,944 psi). The predicted optimum formulation was validated experimentally. The experimental conditions were maintained to ensure fair comparison between the predicted and validated values. The compressive strength test was conducted at the optimum NaOH

molarity and GO concentration, and the results are presented in Fig. 7. The experimental compressive strength at the optimum NaOH molarity and GO concentration was 21.25 MPa (3,103 psi). Based on the validated data, the compressive strength was within the tolerance interval of the predicted value, as in the point prediction function in DOE, with an error of 5.1%.

Table 6 Summary of optimization data for Phase 1

Parameter	Goal	Experimental region		Optimized Condition
		Lower	Upper	
NaOH Molarity (M)	In range	3	5	3.83
GO Concentration (% bwof)	In range	0.2	1.1	0.2
Compressive Strength (psi)	Maximize	1144	2957	2944

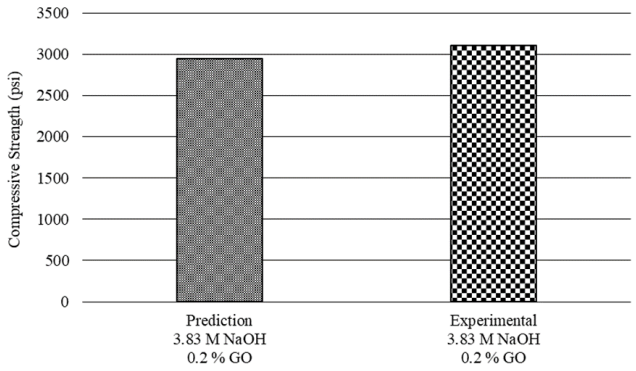

Fig. 7 Prediction and experimental compressive strength of Formulation OP 1 (developed by the authors)

3.2. Adaptability of the Optimum Formulation to Oil Well Cement Functional Tests

The optimum formulation of 3.83 M NaOH and 0.2% GO (Formulation OP 1) was evaluated using oil-well cement functional tests. The aim of this test was to determine the optimal formulation performance in terms of rheology, fluid loss, and thickening time.

3.2.1. Rheology

Table 7 summarizes the rheological measurements of Formulation OP1 conducted at two different temperatures: ambient and 90°C. The rheological properties were evaluated in terms of the material resistance to flow under varying rotational speeds, measured in revolutions per minute (RPM), during both ramp-down and ramp-up sequences. The “Ramp Down” column represents the viscosity measured while decreasing the RPM, whereas the “Ramp Up” column represents the viscosity measured while increasing the RPM. The ratio of “Ramp Up” to “Ramp Down” was calculated to assess the thixotropic or rheopectic nature of the formulation. At ambient temperature, the results indicate an increase in the ratio as the RPM decreases from 200 to 100, suggesting slight thixotropic behavior, where the material becomes less viscous under shear (as indicated by a ratio slightly above 1). At lower RPMs (6 and 3), the ratios normalized to 1, signifying no significant thixotropic or rheopectic behavior, which implies that the material exhibits Newtonian flow characteristics at very low shear rates.

Table 7 Rheology of the Formulation OP 1 at surface temperature and 90 °C (developed by the authors)

RPM	Ambient temperature			90 °C		
	Ramp Down	Ramp Up	Ratio	Ramp Down	Ramp Up	Ratio
300	47	47	1	27	27	1
200	28	29	1.04	21	22	1.05
100	18	19	1.06	16	17	1.06
6	5	5	1	8	8	1
3	4	4	1	7	7	1

When subjected to an elevated temperature of 90°C, the formulation exhibits a consistently lower viscosity across all RPMs, as shown by the “Ramp Down” and “Ramp Up” values, which are significantly lower than those at ambient temperature. The observed reduction in viscosity at higher temperatures is expected due to the decrease in intermolecular forces within the formulation. However, the ratios remain approximately the same, with a slight thixotropy observed at 200 RPM (ratio of 1.05) and otherwise Newtonian behavior (ratios of 1). The uniform ratio across temperatures suggests that the temperature increase does not significantly alter the thixotropic nature of the formulation. The rheological properties presented in Table 7 provide insights into the molecular structure and interactions of the formulation. The slight thixotropy at certain shear rates could be due to reversible structural arrangements in the material, which warrants further investigation, possibly through microscopic or spectroscopic methods, to elucidate the underlying mechanisms.

The rheological assessment of Formulation OP 1 demonstrated its stable flow behavior with slight thixotropic characteristics at specific shear rates and a tendency toward Newtonian behavior at lower shear rates and elevated temperatures. These encouraging rheological finding are consistent with recent studies that observed a decrease in plastic viscosity and an increase in yield points for drilling fluids incorporating GO [33].

3.2.2. Fluid Loss

Formulation OP 1 produced a filtrate volume of 734.2 ml. The relatively high fluid volume in this context could suggest several aspects:

- Insufficient Viscosity: The fluid may not be sufficiently viscous to maintain its integrity under pressure. The NaOH molarity influences the dissolution of silicates and aluminates involved in the polymerization reaction to form the geopolymer matrix. If the molarity is not optimized, it may not provide sufficient viscosity to the system, thereby allowing more fluid to escape.
- Inadequate GO Function: At a concentration of 0.2%, GO might not be effectively filling the void spaces or acting as a suitable reinforcement within the geopolymer matrix, which could be necessary to prevent fluid loss. GO role in cementitious materials often includes improving their mechanical properties and reducing their permeability; however, the effectiveness of this can be highly concentration dependent.
- Pore Structure and Distribution: The fluid loss value reflects the pore structure of the set cement. A higher fluid loss might indicate a more porous structure, which could be due to the NaOH molarity and GO concentration not promoting optimal geopolymerization and pore refinement.

However, the optimal design did not include a fluid loss additive, which is typically employed in cementing applications. The addition of a fluid loss additive and GO can potentially decrease the filtrate volume, thus aligning them with the governance standard.

3.2.3. Thickening Time

The thickening time of a cementitious material, such as that in Formulation OP 1, is a critical parameter in the setting process, representing the transition from a fluid-like state to a semisolid state. It is often reported at different consistency levels measured in Bearden units of consistency (Bc), such as 40, 70, and 100 Bc, which correspond to increasing degrees of thickening. The time required to reach these consistency levels is a key factor in determining the working time and setting characteristics of the material. Fig. 8 illustrates the thickening time of Formulation OP 1 up to 40, 70, and 100 BC.

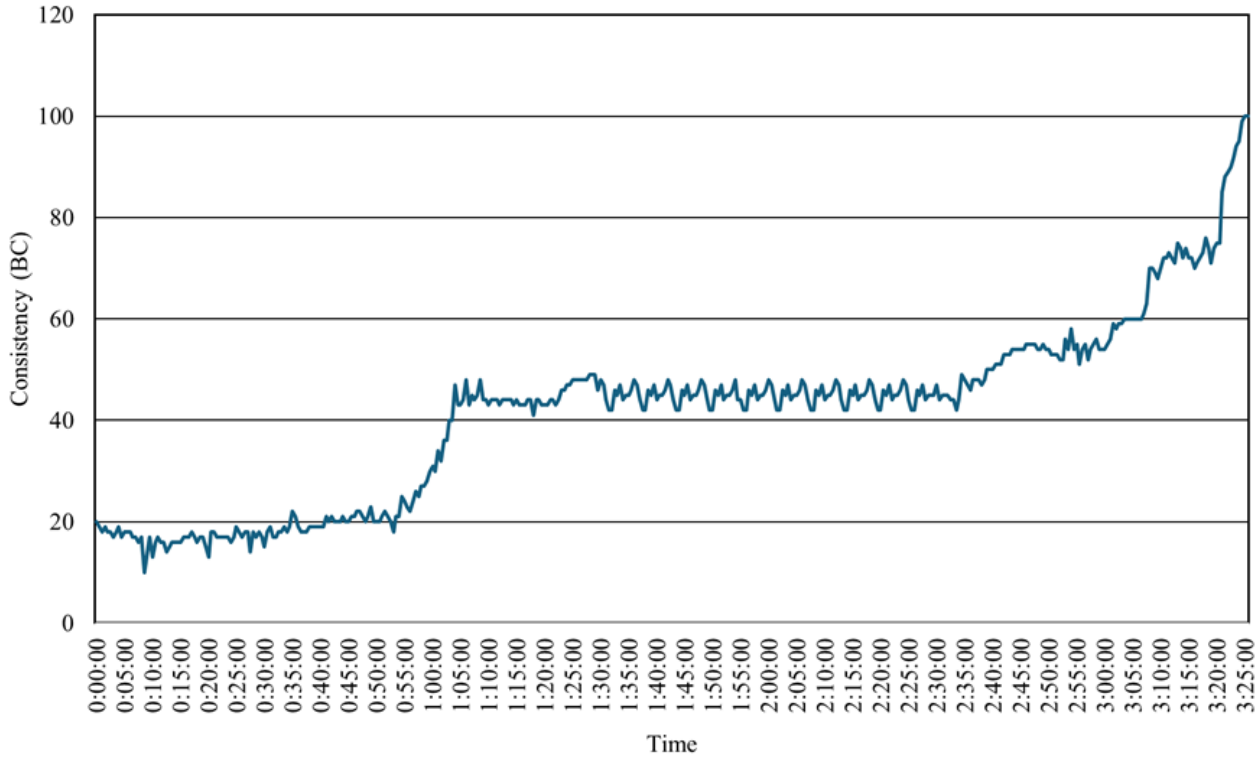

Fig. 8 Thickening time of Formulation OP 1 (developed by the authors)

The reported thickening times for Formulation OP 1—1:03 h (40 Bc), 3:08 h (70 Bc), and 3:25 h (100 Bc)—indicate the progression of the setting process under test conditions. Below is a detailed discussion of each stage:

- Forty Bc at 1:03 h:hr: 40 Bc in just over an hour suggests that Formulation OP 1 begins to lose its fluidity relatively quickly. This level of consistency indicates the initial setting phase, during which the material can no longer be pumped or placed easily. In practical applications, such as well cementing, a relatively short period is required for placement before significant thickening occurs.
- Seventy Bc at 3:08 h: Achieving 70 Bc after approximately three hours indicates a moderate rate of thickening, which allows for some workability during this period. The intermediate consistency level is often associated with the time frame within which the material is in place and begins to bear structural loads. Formulation OP 1 provides a sufficient window for most

applications requiring time for manipulation and positioning.

- One hundred Bc at 3:25 h: The progression from 70 to 100 Bc in approximately 17 min is relatively rapid. This sharp increase indicates a critical point at which material transitions to a near-solid state, losing its plasticity and becoming capable of sustaining substantial loads. The close timing between reaching 70 Bc and 100 Bc suggests a quick transition from a workable state to a set state, which could be critical for operations that require precise timing

In conclusion, the thickening-time data for Formulation OP 1 indicates a formulation that sets relatively quickly, which may be advantageous in scenarios in which early strength development is desired. However, the rapid transition from 70 to 100 Bc suggests that careful consideration must be given to operational timing to ensure proper placement and avoid premature setting. Further research could explore the influence of different variables on the thickening time to fine-tune the formulation for specific applications, ensuring that the formulation delivers the desired performance in terms of the setting time and strength development.

3.3. Effects of Pressure and Temperature on the Compressive Strength of Geopolymers

Phase 3 of the study investigated the effect of pressure and temperature on the geopolymer's compressive strength using the Formulation OP 1. The results are summarized in Table 4. Based on the results obtained, a linear regression model was developed. The ANOVA results for various temperatures and pressures are presented in Table 8. Eq. (4) expresses the empirical model of compressive strength (CS), which indicates the relationship between temperature and pressure in actual factors.

$$CS = 1000 + 15A - 0.9B + 0.01AB \quad (4)$$

where A and B represent temperature and pressure, respectively.

Table 8 ANOVA for the polynomial model in Eq. (4) (developed by the authors)

Response	Source	SS	DF	MS	*F*-value	*p*-value
Compressive Strength	Model	6.12×10^6	3	2.04×10^6	248.97	<0.0001
	Error	1.90×10^4	10	4.75×10^3		

*SS: Sum of squares; DF: Degree of freedom; MS: Mean square

ANOVA findings show that the obtained model gives very high R^2, adjusted R^2, and predicted R^2 values of 0.99, 0.99, and 0.95, respectively. Fig. 9 demonstrates the effectiveness of the predictive model for the compressive strength of fly ash-based geopolymer cement.

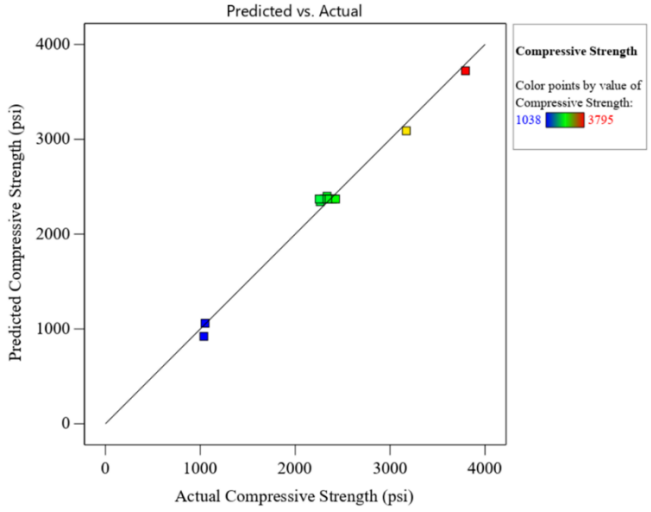

Fig. 9 Predicted versus actual values plotted by the Design Expert for the compressive strength of Phase 3 (developed by the authors)

The strong correlation between the predicted and actual values validates the model application for future material design and optimization. As can be seen, there is a strong alignment for most of the points, which suggests that the model has a substantial predictive capability. Meanwhile, the scatter of points along the entire range of the graph suggests that the model's predictive validity extends across the full spectrum of tested compressive strength values, from lower to higher values. Therefore, the obtained model provides a satisfactory estimation of the predicted values and can be used to predict compressive strength.

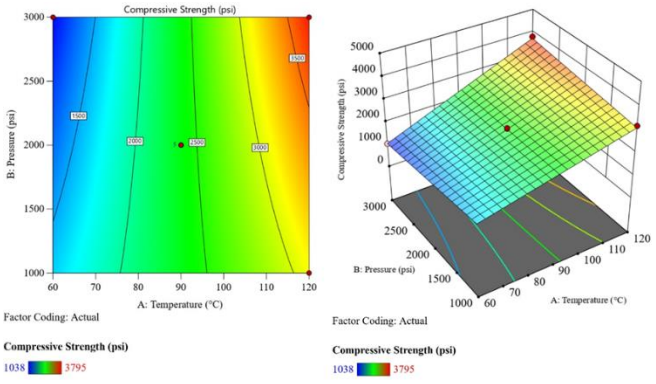

Fig. 10 Contour and 3D response surface plots of compressive strength versus temperature and pressure (developed by the authors)

The contour and 3D response surface plots (Fig. 10) elucidate the variation in compressive strength, which is the dependent variable, as a function of temperature and pressure. The experimental data were mapped onto a contour plot, where the compressive strength values ranged from 7.16 MPa (1,038 psi) to 26.17 MPa (3,795 psi), as shown through a color gradient transitioning from blue (indicative of lower strength) to red

(representing higher strength). The contours, representing lines of constant compressive strength, become denser in regions of higher temperature and pressure, signifying a steep gradient and, thus, substantial sensitivity of compressive strength to changes in these curing conditions. Of particular interest is the region delineated by the highest compressive strength values, which is indicated by the red end of the spectrum. A distinct trend was observed within the design space, where an increase in both curing temperature and pressure contributed to a notable enhancement in the compressive strength of the geopolymer cement. These results suggest that higher temperatures may enhance the chemical processes responsible for strength development in geopolymers. This result is in agreement with several other researchers [10], [34], [35]. This phenomenon is due to high heat curing allowing for more reactivity in the fly ash, which causes more dissolution of the ash and more Al^{3+} and Si^{4+} ions to form a stronger geopolymer. Elevated curing temperatures also allow for the release of water from the geopolymer system, resulting in a less porous and denser geopolymer. This resulted in a product that could withstand greater compressive stress [35].

At a constant temperature, an increase in pressure generally corresponds to an increase in compressive strength. For instance, at 120°C, the strength at 6.90 MPa (1,000 psi) was 21.87 Mpa (3,171 psi), and at 20.68 Mpa (3,000 psi), it increased to 25.83 Mpa (3,745 psi). However, the increase in pressure did not significantly affect the strength when cured at temperature 60°C and 90°C. For example, at 60°C, increasing the pressure from 6.90 Mpa (1,000 psi) to 21.87 Mpa (3,000 psi) only increases the strength by approximately 0.4%. Increasing the curing pressure from 4.04 Mpa (586 psi) to 23.54 Mpa (3,414 psi) at 90°C only increased the strength by 3%. Thus, this could suggest that at lower temperature, the effect of pressure is not as pronounced. The influence of temperature and pressure on the compressive strength can be scientifically reasoned by considering the geopolymerization process, where the molecular structure of the cement is altered through a chemical reaction. Higher temperatures can enhance the dissolution of fly ash particles and the subsequent geopolymerization reaction, leading to denser and more robust microstructures. Similarly, increased pressure can promote a more compact packing of the material, reducing its porosity and increasing its compressive strength. The presence of GO in the mixture was intended to further enhance the mechanical properties of the geopolymer cement. GO, even at low concentrations, can act as a reinforcing agent, improving the stress distribution and crack resistance of the material.

Table 9 lists the optimized pressure and temperature values for Formulation OP 1 to maximize the compressive strength. During the optimization process, both temperature and pressure were set in the ranges of 60–120°C and 6.90 Mpa (1,000 psi) to 20.68 Mpa (3,000 psi), respectively. It can be observed from the table that the established optimum temperatures and pressures were 120°C and 20.68 Mpa (3,000 psi), respectively. Under this optimal condition, the predicted compressive strength is 25.68 Mpa (3,723 psi). The predicted optimum condition was validated, and the compressive strength tests after 24 h are presented in Fig. 11. The experimental compressive strength at the optimum temperature and pressure was 23.83 Mpa (3,455 psi). Based on the validated data, the compressive strength was within the tolerance interval of the predicted value, as in the point prediction function in DOE, with an error of 7.2%.

Table 9 Summary of optimization data for Phase 3 (developed by the authors)

Parameter	Goal	Experimental region		Optimized Condition
		Lower	Upper	
Temperature (°C)	In range	60	120	120
Pressure (psi)	In range	1000	3000	3000
Compressive Strength (psi)	Maximize	1038	3795	3723

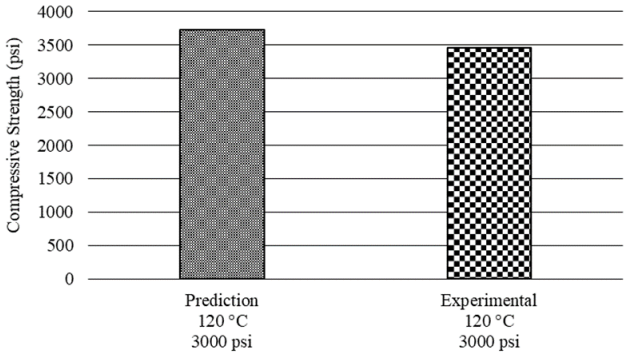

Fig. 11 Prediction and experimental compressive strength at optimal temperature and pressure (developed by the authors)

4. Conclusion

The study was conducted to optimize the graphene concentration to enhance the performance of the fly ash-based geopolymer cement under HPHT conditions for well-cement applications. Concerning the objective of the study, the major findings are summarized below:

1. The study highlighted a nuanced relationship between NaOH molarity, GO concentration, and geopolymer cement compressive strength, revealing optimal results at 3.83 M NaOH and 0.2% GO (Formulation OP 1), achieving a compressive strength of 21.25 MPa. The results identified a threshold effect where high GO concentrations could detrimentally affect strength, emphasizing the importance of balanced formulations for enhanced mechanical properties.

2. Formulation OP 1 underwent rigorous oil-well cement functional tests to evaluate rheology, fluid loss, and thickening time, which are pivotal for applying lab results to field scenarios. Rheological assessments indicated thixotropic behavior at ambient temperatures and consistently lower viscosities at 90°C, suggesting potential for real-world applications despite the high filtrate volume of 734.2 ml in fluid loss tests, which can be attributed to the absence of a fluid loss additive. The formulation's thickening time suggests that it sets relatively quickly, which highlights the need for precise operational timing in practical applications.

3. Variations in pressure and temperature affect the compressive strength of fly ash-based geopolymer cement. The study confirmed that compressive strength significantly increases with temperature due to enhanced fly ash reactivity, which promotes a denser, more robust geopolymer structure, whereas the impact of pressure on strength was less marked, suggesting that temperature plays a more critical role in geopolymerization and strength enhancement. The optimal compressive strength was achieved at 120°C and 3,000 psi, with experimental results closely aligning with predictions, indicating the formulation effectiveness under challenging conditions typical of oil well cementing applications.

In conclusion, the incorporation of GO at optimal concentrations can significantly improve the performance of geopolymer cements at elevated pressures and temperatures. The functional tests demonstrated that the properties of GO are crucial for enhancing the geopolymer well cement performance. GO serves as a multifunctional additive that enhances the rheological properties, reduces fluid loss volume, and shortens the thickening time of geopolymer cement. While GO has been extensively studied in concrete applications, its use in geopolymer cement across a wider range of pressures and temperatures provides valuable insights into the oil and gas industry.

Nevertheless, due to time and cost constraints, the present study has some limitations. The study was conducted without incorporating other commercial functional additives, and the compressive strength tests were short-term, demonstrating only the initial compressive strength development. Additionally, the study focused solely on GO without comparing its effects with those of reduced graphene oxide. Future research should address these limitations to provide a more comprehensive understanding of GO's impact on well-cement performance.

Recommendations

1. Further studies should incorporate functional additives such as rheology modifiers, fluid loss additives, retarders, and accelerators. The addition of additives helps fine-tune the results to meet the specific requirements of well operations.

2. To conduct compatibility tests between commercial functional additives and GO. Understanding the interactions and compatibility of the additives can provide insights into optimizing the formulation for enhanced performance.

3. While the present study examined the effects of different pressures and temperatures on compressive strength, future research should focus on the impact of longer curing durations. This will help observe the long-term effects of the additives on the performance of the geopolymer well cement and identify potential degradation over time.

4. The present study provides an opportunity to investigate the use of reduced graphene oxide as a substitute for current GO. Reduced graphene oxide may enhance the performance of geopolymer well cements under elevated pressures and temperatures.

5. To perform a cost analysis to evaluate the economic feasibility of graphene oxide compared with commercial additives. The performance benefits should be balanced against the higher cost of graphene oxide to determine its viability for widespread application.

Acknowledgments

This research was funded by PETRONAS Research Sdn. Bhd., Malaysia via project cost center E.025.GST.02019.003, as per the record of PETRONAS Research Sdn. Bhd.

References

[1] BENSTED J. Class G and H Basic Oilwell Cements. *World Cement*, 1992, (April): 44-50.

[2] NASVI M. C. M., RANJITH P. G., and SANJAYAN J. Comparison of Mechanical Behaviors of Geopolymer and Class G Cement as Well Cement at Different Curing Temperatures for Geological Sequestration of Carbon Dioxide. *Paper presented at the 46th U.S. Rock Mechanics/Geomechanics Symposium*, Chicago, Illinois, June 24-27, 2012.

[3] NASVI M. C. M., GAMAGE R. P., and JAY S. Geopolymer as Well Cement and the Variation of Its Mechanical Behavior with Curing Temperature. *Greenhouse Gases: Science and Technology,* 2012, 3(1): 46-58. https://doi.org/10.1002/ghg.39.

[4] RIDHA S., ABD HAMID A. I., SETIAWAN R. A., IBRAHIM M. A., and SHAHARI A. R. Microstructure Behavior of Fly Ash-Based Geopolymer Cement Exposed to Acidic Environment for Oil Well Cementing. *Arabian Journal for Science and Engineering*, 2018, 43(11): 6413-6428. https://doi.org/10.1007/s13369-018-3183-5.

[5] ZHANG W., ZHANG Y., and GAO L. Effect of Low-Calcium Fly Ash on Sulfate Resistance of Cement Paste under Different Exposure Conditions. *Advances in Concrete Construction*, 2019, 7(3): 175-181. https://doi.org/10.12989/acc.2019.7.3.175.

[6] SHARONOVA O. M., SOLOVYOV L. A., and ANSHITS A. G. The Influencing Factors for the Strength Enhancement of Composite Materials Made Up of Fine High-Calcium Fly Ash. *Advances in Concrete Construction*, 2023, 16(3): 169-176. https://doi.org/10.12989/acc.2023.16.3.169.

[7] KURTOGLU A. E., et al. Mechanical and Durability Properties of Fly Ash and Slag Based Geopolymer Concrete. *Advances in Concrete Construction*, 2018, 6(4): 345-362. https://doi.org/10.12989/acc.2018.6.4.345.
[8] DAVIDOVITS J. Properties of Geopolymer Cements. *First international conference on alkaline cements and concretes*, Place, 1994, pp. 131-149.
[9] ABDULLAH M. M. A. B., KAMARUDIN H., ABDULKAREEM O. A. K. A., GHAZALI C. M. R., RAFIZA A. R., and NORAZIAN N. Optimization of Alkaline Activator/Fly ASH Ratio on the Compressive Strength of Manufacturing Fly Ash-Based Geopolymer. *Applied Mechanics and Materials*, 2012, 110-116: 734-739. https://doi.org/10.4028/www.scientific.net/AMM.110-116.734.
[10] ABDULLAH M. M. A. B., KAMARUDIN H., BNHUSSAIN M., ISMAIL K. N., RAFIZA A. R., and ZARINA Y. The Relationship of NaOH Molarity, Na_2SiO_3/NaOH Ratio, Fly Ash/Alkaline Activator Ratio, and Curing Temperature to the Strength of Fly Ash-Based Geopolymer. *Advanced Materials Research*, 2012, 328-330: 1475-1482. https://doi.org/10.4028/www.scientific.net/AMR.328-330.1475.
[11] LIU B., TAN J., SHI H., LIANG H., JIANG J., and YANG Y. Effect of Sulfate Activators on Mechanical Property of High Replacement Low-Calcium Ultrafine Fly Ash Blended Cement Paste. *Advances in Concrete Construction*, 2021, 11(3): 183-192. https://doi.org/10.12989/acc.2021.11.3.183.
[12] HOSSEINI S. A. Seawater Curing Effects on the Permeability of Concrete Containing Fly Ash. *Advances in Concrete Construction*, 2022, 14(3): 205-214. https://doi.org/10.12989/acc.2022.14.3.205.
[13] UDEZE O. J., MOHAMMED B. S., ADEBANJO A. U., and ABDULKADIR I. Optimizing an Eco-Friendly High-Density Concrete for Offshore Applications: A Study on Fly Ash Partial Replacement and Graphene Oxide Nano Reinforcement. *Case Studies in Chemical and Environmental Engineering*, 2024, 9: 100592. https://doi.org/10.1016/j.cscee.2023.100592.
[14] BHEEL N., ALI M. O. A., KIRGIZ M. S., SHAFIQ N., and GOBINATH R. Effect of graphene oxide particle as nanomaterial in the production of engineered cementitious composites including superplasticizer, fly ash, and polyvinyl alcohol fiber. *Materials Today: Proceedings*, Published online March 8, 2023. https://doi.org/10.1016/j.matpr.2023.03.010.
[15] SAJJAD U., SHEIKH M. N., and HADI M. N. S. Incorporation of Graphene in Slag-Fly Ash-Based Alkali-Activated Concrete. *Construction and Building Materials*, 2022, 322: 126417. https://doi.org/10.1016/j.conbuildmat.2022.126417.
[16] DU S., JIANG Y., ZHONG J., GE Y., and SHI X. Surface Abrasion Resistance of High-Volume Fly Ash Concrete Modified by Graphene Oxide: Macro- and Micro-Perspectives. *Construction and Building Materials*, 2020, 237: 117686. https://doi.org/10.1016/j.conbuildmat.2019.117686.
[17] BELLUM R. R., MUNIRAJ K., INDUKURI C. S. R., and MADDURU S. R. C. Investigation on Performance Enhancement of Fly ash-GGBFS Based Graphene Geopolymer Concrete. *Journal of Building Engineering*, 2020, 32: 101659. https://doi.org/10.1016/j.jobe.2020.101659.
[18] GAO Y., JING H., FU G., ZHAO Z., and SHI X. Studies on Combined Effects of Graphene Oxide-Fly Ash Hybrid on the Workability, Mechanical Performance and Pore Structures of Cementitious Grouting under High W/C Ratio. *Construction and Building Materials*, 2021, 281: 122578. https://doi.org/10.1016/j.conbuildmat.2021.122578.
[19] MOHANTA Y., BISWAS K., MAHANTA S., and MUTHUPANDIAN S. *Graphene-Based Nanomaterials: Application in Food, Agriculture and Healthcare.* Boca Raton: CRC Press, 2023.
[20] HAO S., CHENG Y., and YUBIN C. *Graphene Composite Materials (Graphene Composite Materials)*. Singapore: World Scientific Publishing Co. Pte. Ltd., 2023.
[21] LI W., LI X., CHEN SHU J., LONG G., LIU YAN M, and DUAN WEN, H. Effects of Nanoalumina and Graphene Oxide on Early-Age Hydration and Mechanical Properties of Cement Paste. *Journal of Materials in Civil Engineering*, 2017, 29(9): 04017087. https://doi.org/10.1061/(ASCE)MT.1943-5533.0001926.
[22] AMERICAN PETROLEUM INSTITUTE (API). *API RP-10B2: Recommended Practice for Testing Well Cements*. 2nd ed. Washington, DC, USA, 2019.
[23] AMERICAN PETROLEUM INSTITUTE (API). *API RP10B-5: Recommended Practice on Determination of Shrinkage and Expansion of Well Cement Formulations at Atmospheric Pressure*. Washington, DC, USA, 2005.
[24] PETRONAS. *PETRONAS Technical Guidelines – Cementing (Volume PTG 25.01.04)*. Kuala Lumpur, Malaysia, 2016.
[25] PIKŁOWSKA A. Rheological Properties of Cement Slurries Modified by Silica Nanostructures Applied in Drilling Industry. *E3S Web of Conferences*, 2018, 71: 00012. https://doi.org/10.1051/e3sconf/20187100012.
[26] PLANK J., SCHROEFL C., GRUBER M., LESTI M., and SIEBER R. Effectiveness of Polycarboxylate Superplasticizers in Ultra-High Strength Concrete: The Importance of PCE Compatibility with Silica Fume. *Journal of Advanced Concrete Technology*, 2009, 7(1): 5-12. https://doi.org/10.3151/jact.7.5.
[27] CHALAH K., MAHDAD M. H., BENMOUNAH A., KHERIBET R., and AKOUCHE A. Effect of Silica Fume on Cement Rheology Properties in Presence of Superplasticisers. *Materials Today: Proceedings*, 2022, 58: 1246-1250. https://doi.org/10.1016/j.matpr.2022.02.006.
[28] CHINTALAPUDI K. and PANNEM R. M. R. Enhanced Strength, Microstructure, and Thermal Properties of Portland Pozzolana Fly Ash-Based Cement Composites by Reinforcing Graphene Oxide Nanosheets. *Journal of Building Engineering*, 2021, 42: 102521. https://doi.org/10.1016/j.jobe.2021.102521.
[29] BAYER İ. R. Graphene Oxide-Reinforced Cementitious Concrete Composites that Incorporates Silica Fume and Fly Ash. *International Journal of Engineering Research and Development (in EN)*, 2023, 15(2): 526-534. https://doi.org/10.29137/umagd.1258578.
[30] LU Z., HOU D., MENG L., SUN G., LU C., and LI Z. Mechanism of Cement Paste Reinforced by Graphene Oxide/Carbon Nanotubes Composites with Enhanced Mechanical Properties. *RSC Advances*, 2015, 5(122): 100598-100605. https://doi.org/10.1039/C5RA18602A.
[31] YANG H., MONASTERIO M., CUI H., and HAN N. Experimental Study of the Effects of Graphene Oxide on Microstructure and Properties of Cement Paste Composite.

Composites Part A: Applied Science and Manufacturing, 2017, 102: 263-272. https://doi.org/10.1016/j.compositesa.2017.07.022.
[32] SHAMSAEI E., DE SOUZA F. B., YAO X., BENHELAL E., AKBARI A., and DUAN W. Graphene-Based Nanosheets for Stronger and More Durable Concrete: A review. *Construction and Building Materials*, 2018, 183: 642-660. https://doi.org/10.1016/j.conbuildmat.2018.06.201.
[33] IKRAM R., JAN B. M., AHMAD W., SIDEK A., KHAN M., and KENANAKIS G. Rheological Investigation of Welding Waste-Derived Graphene Oxide in Water-Based Drilling Fluids. *Materials*, 2022, 15(22): 8266. https://doi.org/10.3390/ma15228266.
[34] CHINDAPRASIRT P., CHAREERAT T., and SIRIVIVATNANON V. Workability and Strength of Coarse High Calcium Fly Ash Geopolymer. *Cement and Concrete Composites*, 2007, 29(3): 224-229. https://doi.org/10.1016/j.cemconcomp.2006.11.002.
[35] GENEKE T. *Effect of Alkaline Activator Composition on the Geopolymer Properties Produced from South African Power Station Fly Ash*. Master of Engineering in Chemical Engineering, Chemical Engineering Department, North West University, Potchefstroom, South Africa, 2021.

参考文:

[1] BENSTED J. G 级和 H 级基础油井水泥。世界水泥，1992，（4 月）：44-50。
[2] NASVI M. C. M.、RANJITH P. G. 和 SANJAYAN J. 地质聚合物和 G 级水泥作为油井水泥在不同固化温度下的力学行为比较，用于二氧化碳的地质封存。论文发表于第 46 届美国岩石力学/地质力学研讨会，伊利诺伊州芝加哥，2012 年 6 月 24 日至 27 日。
[3] NASVI M. C. M.、GAMAGE R. P. 和 JAY S. 地质聚合物作为油井水泥及其力学行为随固化温度的变化。温室气体：科学与技术，2012，3(1)：46-58。https://doi.org/10.1002/ghg.39。
[4] RIDHA S.、ABD HAMID A. I.、SETIAWAN R. A.、IBRAHIM M. A. 和 SHAHARI A. R. 酸性环境下油井固井用粉煤灰基土聚物水泥的微观结构行为。《阿拉伯科学与工程杂志》，2018，43(11)：6413-6428。https://doi.org/10.1007/s13369-018-3183-5。
[5] ZHANG W., ZHANG Y., and GAO L. 不同暴露条件下低钙粉煤灰对水泥浆体抗硫酸盐性能的影响。《混凝土建设进展》，2019，7(3)：175-181。https://doi.org/10.12989/acc.2019.7.3.175。
[6] SHARONOVA O. M.、SOLOVYOV L. A. 和 ANSHITS A. G. 高钙细粉煤灰复合材料强度提高的影响因素。混凝土建设进展，2023，16(3): 169-176。https://doi.org/10.12989/acc.2023.16.3.169。
[7] KURTOGLU A. E. 等。粉煤灰和矿渣基土聚物混凝土的力学性能和耐久性。混凝土建设进展，2018，6(4): 345-362。https://doi.org/10.12989/acc.2018.6.4.345。
[8] DAVIDOVITS J. 土聚物水泥的性能。第一届碱性水泥和混凝土国际会议，Place，1994，第 131-149 页。
[9] ABDULLAH M. M. A. B.、KAMARUDIN H.、ABDULKAREEM O. A. K. A.、GHAZALI C. M. R.、RAFIZA A. R. 和 NORAZIAN N. 优化碱性活化剂/粉煤灰比例对粉煤灰基土聚合物制造抗压强度的影响。应用力学与材料，2012，110-116：734-739。https://doi.org/10.4028/www.scientific.net/AMM.110-116.734。
[10] ABDULLAH M. M. A. B.、KAMARUDIN H.、BNHUSSAIN M.、ISMAIL K. N.、RAFIZA A. R. 和 ZARINA Y. NaOH 摩尔浓度、Na2SiO3/NaOH 比、粉煤灰/碱性激发剂比和固化温度与粉煤灰基土聚物强度的关系。先进材料研究，2012，328-330：1475-1482。https://doi.org/10.4028/www.scientific.net/AMR.328-330.1475。
[11] LIU B., TAN J., SHI H., LIANG H., JIANG J., 和 YANG Y.。硫酸盐激发剂对高取代低钙超细粉煤灰混合水泥浆体力学性能的影响。混凝土施工进展，2021，11(3): 183-192。https://doi.org/10.12989/acc.2021.11.3.183。
[12] HOSSEINI S. A. 海水养护对含粉煤灰混凝土渗透性的影响。混凝土施工进展，2022，14(3): 205-214。https://doi.org/10.12989/acc.2022.14.3.205。
[13] UDEZE O. J.、MOHAMMED B. S.、ADEBANJO A. U. 和 ABDULKADIR I. 优化用于海上应用的环保高密度混凝土：粉煤灰部分替代和氧化石墨烯纳米增强的研究。化学与环境工程案例研究，2024，9：100592。https://doi.org/10.1016/j.cscee.2023.100592。
[14] BHEEL N.、ALI M. O. A.、KIRGIZ M. S.、SHAFIQ N. 和 GOBINATH R. 氧化石墨烯颗粒作为纳米材料在生产工程水泥基复合材料（包括高效减水剂、粉煤灰和聚乙烯醇纤维）中的作用。当今材料：会议录，2023 年 3 月 8 日在线发表。https://doi.org/10.1016/j.matpr.2023.03.010。
[15] SAJJAD U.、SHEIKH M. N. 和 HADI M. N. S. 石墨烯在矿渣粉煤灰基碱激活混凝土中的应用。建筑与建筑材料，2022，322：126417。https://doi.org/10.1016/j.conbuildmat.2022.126417。
[16] DU S.、JIANG Y.、ZHONG J.、GE Y. 和 SHI X. 氧化石墨烯改性高掺量粉煤灰混凝土的表面耐磨性：宏观和微观视角。建筑与建筑材料，2020，237：117686。https://doi.org/10.1016/j.conbuildmat.2019.117686。
[17] BELLUM R. R.、MUNIRAJ K.、INDUKURI C. S. R. 和 MADDURU S. R. C. 粉煤灰-GGBFS 基石墨烯土聚物混凝土性能增强研究。建筑工程杂志，2020，32：101659。https://doi.org/10.1016/j.jobe.2020.101659。
[18] GAO Y., JING H., FU G., ZHAO Z., 和 SHI X。高水灰比下氧化石墨烯-粉煤灰混合物对胶凝灌浆可加工性、

力学性能及孔隙结构的综合影响研究。建筑与建筑材料，2021，281：122578。https://doi.org/10.1016/j.conbuildmat.2021.122578。
[19] MOHANTA Y.、BISWAS K.、MAHANTA S. 和 MUTHUPANDIAN S. 石墨烯基纳米材料：在食品、农业和医疗保健中的应用。博卡拉顿：CRC Press，2023。
[20] HAO S., CHENG Y., 和 YUBIN C. 石墨烯复合材料 (Graphene Composite Materials). 新加坡：世界科学出版有限公司，2023。
[21] LI W., LI X., CHEN SHU J., LONG G., LIU YAN M, 和 DUAN WEN, H. 纳米氧化铝和氧化石墨烯对水泥浆体早期水化和力学性能的影响。土木工程材料杂志，2017，29(9)：04017087。https://doi.org/10.1061/(ASCE)MT.1943-5533.0001926。
[22] 美国石油学会 (API)。API RP-10B2：测试井水泥的推荐规范。第二版。美国华盛顿特区，2019。
[23] 美国石油学会 (API)。API RP10B-5：大气压下确定井水泥配方收缩和膨胀的推荐做法。美国华盛顿特区，2005。
[24] 马来西亚国家石油公司。马来西亚国家石油公司技术指南 - 固井（第 PTG 25.01.04 卷）。马来西亚吉隆坡，2016。
[25] PIKŁOWSKA A. 二氧化硅纳米结构改性水泥浆在钻井工业中的流变性能。E3S 网络会议，2018，71：00012。https://doi.org/10.1051/e3sconf/20187100012。
[26] PLANK J.、SCHROEFL C.、GRUBER M.、LESTI M. 和 SIEBER R. 聚羧酸减水剂在超高强度混凝土中的有效性：PCE 与硅粉相容性的重要性。《先进混凝土技术杂志》，2009，7(1)：5-12。https://doi.org/10.3151/jact.7.5。
[27] CHALAH K.、MAHDAD M. H.、BENMOUNAH A.、KHERIBET R. 和 AKOUCHE A. 硅粉在存在减水剂的情况下对水泥流变性能的影响。《今日材料》：会议录，2022，58：1246-1250。https://doi.org/10.1016/j.matpr.2022.02.006。
[28] CHINTALAPUDI K. 和 PANNEM R. M. R. 通过增强氧化石墨烯纳米片增强波特兰火山灰基水泥复合材料的强度、微观结构和热性能。《建筑工程杂志》，2021，42：102521。https://doi.org/10.1016/j.jobe.2021.102521。
[29] BAYER İ. R. 掺有硅灰和粉煤灰的氧化石墨烯增强水泥基混凝土复合材料。《国际工程研究与发展杂志》（EN），2023，15(2)：526-534。https://doi.org/10.29137/umagd.1258578。
[30] LU Z., HOU D., MENG L., SUN G., LU C., 和 LI Z. 氧化石墨烯/碳纳米管复合材料增强水泥浆体力学性能的机理. RSC 进展, 2015, 5(122): 100598-100605. https://doi.org/10.1039/C5RA18602A.
[31] YANG H., MONASTERIO M., CUI H., 和 HAN N. 氧化石墨烯对水泥浆体复合材料微观结构与性能影响的实验研究. 复合材料 A 部分：应用科学与制造，2017, 102: 263-272. https://doi.org/10.1016/j.compositesa.2017.07.022.
[32] SHAMSAEI E.、DE SOUZA F. B.、YAO X.、BENHELAL E.、AKBARI A. 和 DUAN W. 基于石墨烯的纳米片用于更坚固耐用的混凝土：综述。建筑与建筑材料，2018，183：642-660。https://doi.org/10.1016/j.conbuildmat.2018.06.201。
[33] IKRAM R.、JAN B. M.、AHMAD W.、SIDEK A.、KHAN M. 和 KENANAKIS G. 水基钻井液中焊接废料衍生氧化石墨烯的流变学研究。材料，2022，15(22)：8266。https://doi.org/10.3390/ma15228266。
[34] CHINDAPRASIRT P.、CHAREERAT T. 和 SIRIVIVATNANON V. 粗粒高钙粉煤灰土聚合物的可加工性和强度。水泥与混凝土复合材料，2007，29(3)：224-229。https://doi.org/10.1016/j.cemconcomp.2006.11.002。
[35] GENEKE T. 碱性活化剂成分对南非发电站粉煤灰生产的土聚合物性能的影响。化学工程硕士，西北大学化学工程系，波切夫斯特鲁姆，南非，2021。